JPE 15-4-8

http://dx.doi.org/10.6113/JPE.2015.15.4.939
ISSN(Print): 1598-2092 / ISSN(Online): 2093-4718

A New Random SPWM Technique for AC-AC Converter-Based WECS

Navdeep Singh* and Vineeta Agarwal†

*†Department of Electrical Engineering, MNNIT Allahabad, India

Abstract

A single-stage AC-AC converter has been designed for a wind energy conversion system (WECS) that eliminates multistage operation and DC-link filter elements, thus resolving size, weight, and reliability issues. A simple switching strategy is used to control the switches that changes the variable-frequency AC output of an electrical generator to a constant-frequency supply to feed into a distributed electrical load/grid. In addition, a modified random sinusoidal pulse width modulation (RSPWM) technique has been developed for the designed converter to make the overall system more efficient by increasing generating power capacity and reducing the effects of inter-harmonics and sub-harmonics generated in the WECS. The technique uses carrier and reference waves of variable switching frequency to calculate the firing angles of the switches of the converter so that the three-phase output voltage of the converter is very close to a sine wave with reduced THD. A comparison of the performance of the proposed RSPWM technique with the conventional SPWM demonstrated that the power generated by a turbine in the proposed approximately increased by 5% to 10% and THD reduces by 40% both in voltage and current with respect to conventional SPWM.

Key words: AC-AC converter, Frequency controller, PMSG, PWM technique, Wind Energy System

I. INTRODUCTION

Environmental contributions such as solar, wind, ocean, and biomass energy affect the production of electricity. For a small wind generator, a permanent magnet synchronous generator (PMSG) is preferred because of its reliability and high efficiency. In a wind energy conversion system (WECS), load specification is achieved using a power electronic converter. Power electronic converters are used to extract the maximum power and control electrical energy at constant frequency and voltage [1]. Various types of converters such as two-level PWM converters, matrix converters, and multilevel converters are described in different literature [2], [3]. These converters are designed to control the output voltage, current, and power for distributed load operation. Two different configurations in literature are reported to convert wind energy into electrical energy. In first configuration (Fig. 1 (a)), PMSG is driven by a turbine and controlled by a controlled rectifier, followed by the DC bus capacitor [4]. In the second configuration (Fig. 1 (b)), the PMSG's power is controlled by a diode bridge and a chopper is used to control the output voltage following the wind pattern [5]. In these configurations, the PMSG effort and converter power capability is lower because of the multistage operation [6].

The multistage operation is solved [7] with the application of a matrix converter consisting of nine bidirectional switches. The advantages of a matrix converter are well-known for grid-connected or distributed load systems. In a distributed load system, the load may be three-phase or single-phase [8]. The power requirement of each single-phase or three-phase load causes unbalance in the three-wire power system. An isolated neutral wire is required to independently control the phase supply voltage to balance a distributed system. In a four-wire load system, a neutral wire is used to allow the zero-sequence current to minimize the unbalanced load effect. Hence the topology of a 3×3 Matrix converter may be replaced with a four-wire single stage AC-AC converter wherein 12 bidirectional switches are required to connect the generator to the four wire outputs [9]-[11].

The improvement in the conversion process is achieved by fixed-time switching patterns based on modulation algorithms such as space vector PWM or carrier-based PWM

Manuscript received Dec. 9, 2014; accepted Apr. 11, 2015
Recommended for publication by Associate Editor Sangshin Kwak.
†Corresponding Author: vineeta@mnnit.ac.in
Tel: +91-9838075072, MNNIT Allahabad
*Department of Electrical Engineering, MNNIT Allahabad, India

[12], [13]. The problem associated with these algorithms is that these are used under normal input voltage conditions at constant frequency. The duty cycles of the power switches are pre-calculated and tabulated to obtain a desired frequency [14], [15]. Under distorted input voltage conditions at variable frequencies, a fixed time strategy is not appropriate because the disturbance on the input side of the converter reflects on the output of the converter [16]. The speed (frequency) variation that occurs in a variable speed generator affects the duty cycles of time switching patterns and creates a complex controller for controlling constraint [17]. Therefore, it is necessary to calculate the duty cycles of switching patterns instantaneously by measuring the output voltages at each sampling period.

During power conversion, the AC-AC converter distorts the output of generator system but is improved using PWM techniques [18]. Until now, several carrier-based PWM strategies are used to improve the THD of the converter. In the existing PWM control switching scheme, the converter switches operation at a higher frequency than the AC line frequency for the LC filter to easily remove the switching. The AC line current waveform can be more sinusoidal at the expense of switching losses [19]. In a variable speed generator system, these PWM techniques are not feasible because of the variation in speed. If input supply varies, the harmonic spectrum, third, fifth, seventh, and inter- and sub-harmonics of the input supply frequency also vary [20]. In a carrier-based modulation technique, the carrier frequency is not considered a rational integer multiple of either the input frequency or the output frequency for harmonics mitigation. Hence proposing a random harmonic elimination technique as an alternative to conventional PWM techniques for variation in the input frequency for an AC-AC converter is challenging [21].

In this paper, a single-stage three-phase to three-phase AC-AC converter with a four-wire system has been proposed for a variable speed wind turbine driving a PMSG that converts variable-frequency AC output of electrical generator into a constant-frequency supply that can be fed into a distributed load, as shown in Fig. 1(c). A single stage AC-AC variable frequency to constant frequency power electronic converter used in WECS has several merits as compared with two-stage converters. In this converter, only three switches are conducted a time whereas a two-stage converter, a minimum of four to six switches conduct in rectification and inversion at a time. The conduction of more switches at a time increases the total loss in the two stages compared with the single stage converter. This improves the efficiency of the proposed converter and resolves size and reliability issues. The direct carrier-based modulation technique is replaced by a modified random sinusoidal pulse width modulation (RSPWM) technique with a variable switching frequency that makes the overall system more efficient by increasing the generated power capacity and reducing the effects of inter and sub-harmonic generated in WECS.

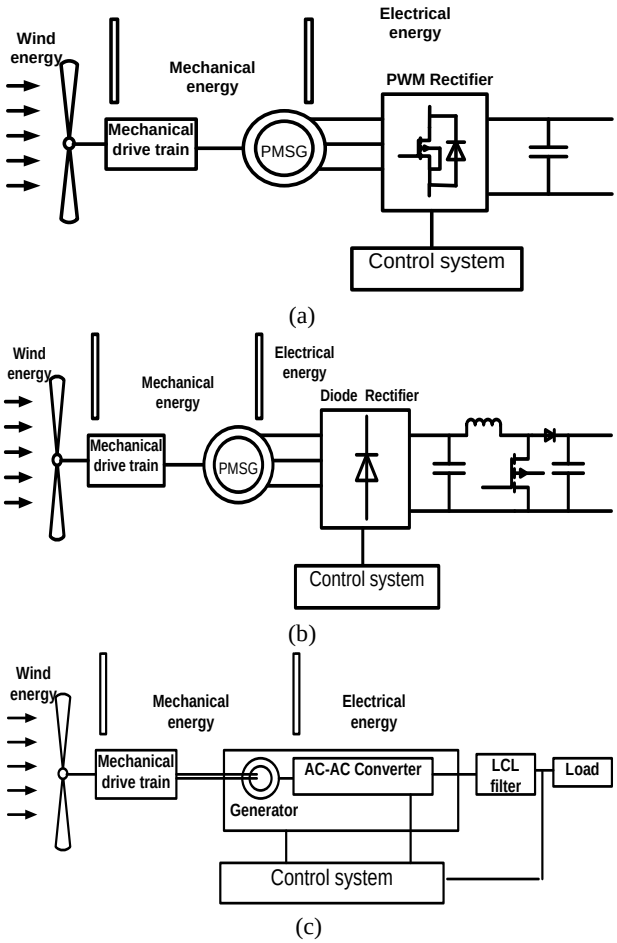

Fig. 1. Different configurations of WECS. (a) Controlled Rectifier AC-DC-AC converter. (b) Diode rectifier and chopper controlled AC-DC-AC converter. (c) AC-AC converter-based wind energy system.

II. Modeling of AC-AC Converter

Fig. 2(a) shows the block diagram of a WECS with a variable frequency to constant frequency three-phase to three-phase AC to AC converter. The side-1 of the converter is connected to the three-phase output of PMSG at frequency f_i and voltage magnitude V_i, whereas a three-phase load is connected on side-2. This converter converts the three-phase balanced sinusoidal voltage on side-1 to a three-phase balanced sinusoidal system on side-2 with new electrical characteristics, frequency f_o and voltage magnitude V_o. The power circuit of a three-phase to three-phase AC to AC converter, connected at the three-phase output of PMSG is depicted in Fig. 2(b). Each of the three converters (PA, PB and PC) functions for one of the three phases. In a steady-state operation, all the three converters are identically operated. Hence it is sufficient to analyze one converter operation because the other converters are symmetrical with a

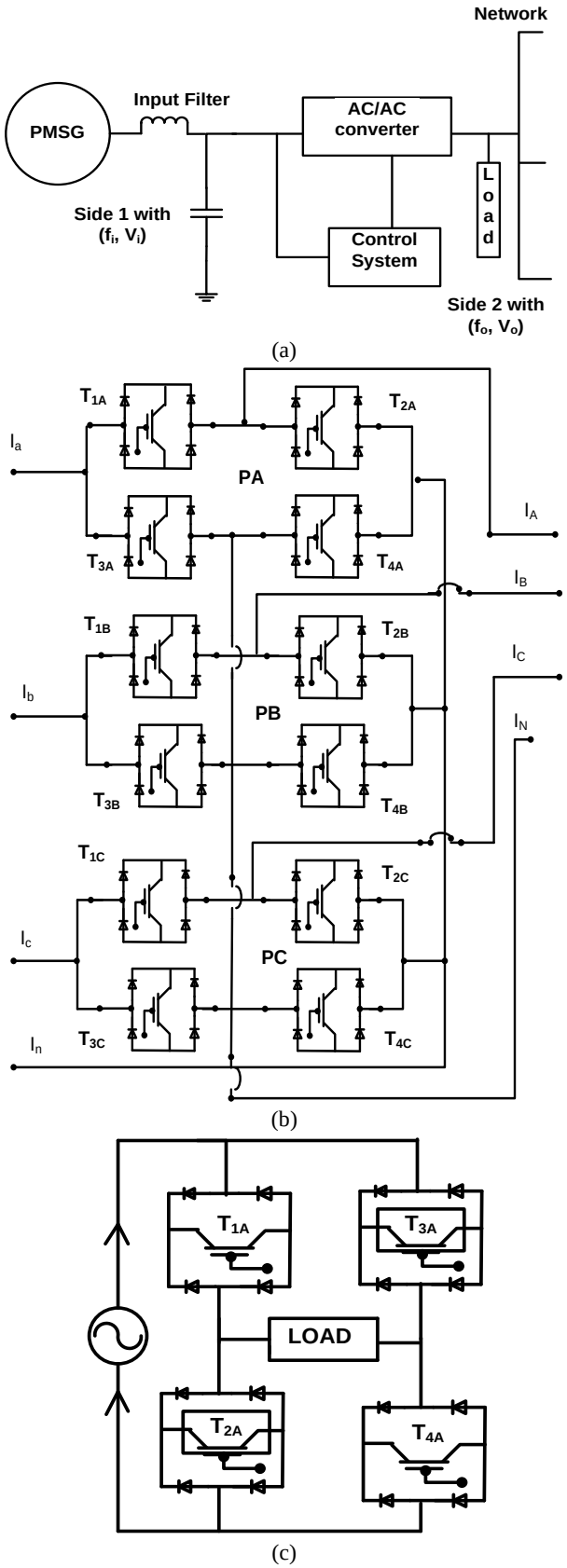

Fig. 2. Wind energy converter topology. (a) Block diagram of 3-Phase AC-AC Converter for WECS. (b) Power circuit of 3-Phase 4- wire AC-AC Converter. (c) Power circuit of single unit converter PA.

TABLE I
TRUTH TABLE FOR TRIGGERING THE SWITCHES

Polarity of Voltage	Switching State of Output Voltage	Switching State of Input Voltage	Conducting Switches
$V_i < 0$ $V_o < 0$	0	0	$T_4 \rightarrow T_1$
$V_i > 0$ $V_o < 0$	0	1	$T_3 \rightarrow T_2$
$V_i < 0$ $V_o > 0$	1	0	$T_2 \rightarrow T_3$
$V_i > 0$ $V_o > 0$	1	1	$T_1 \rightarrow T_4$

phase difference of 120 and 240. Converter PA is redrawn in Fig. 2(c) for a better visualization of its operation.

A. Operation of Converter for Variable Frequency Input Supply

The trigger pulses required for the different switches of converter PA are illustrated in Fig. 3(a). The input signal V_{iA} that is directly proportional to the wind speed has a variable frequency f_i that is, in fact, the output voltage of PMSG.

The signal V_{oA} is at the output frequency f_o of the grid at 50 Hz. These two signals are used to trigger the converter according to the logical switching pattern. Signals G_{1A}, G_{2A}, G_{3A}, and G_{4A} are identified as the trigger signals for the four pairs of switches (T_{1A}, T_{4A}), (T_{2A}, T_{3A}), (T_{4A}, T_{1A}), and (T_{3A}, T_{2A}), respectively. Table 1 shows the truth table for triggering the switches of the converter in Fig. 2(c). In the table, positive output is considered as logic '1', whereas negative output is presented by logic '0'. When both input and output are positive, it is represented by logic '11', and when both are negative it shown as '00'. Thus the switching state will change according to the wind speed and frequency of the output voltage.

B. Switching Strategy for Positive Output Waveform

The converter will produce a positive output when switches T_{1A} and T_{4A} conduct a positive input cycle, whereas switches T_{2A} and T_{3A} conduct a negative input cycle, as shown in Fig. 3(b).

During time period T_{sp1}, T_{1A} and T_{4A} must conduct while the other switches must be turned off. Similarly, during time period T_{sp2}, T_{2A} and T_{3A} must conduct while other switches must be turned off. Thus the output voltage for one positive half output cycle is given by Equation (1),

$$V_o = (T_{sp1} - T_{sp2}) \times V_i \tag{1}$$

$$T_{sp1} = \sum_{n1=1}^{N1} \frac{t_{n1}}{T_s / 2} \tag{2}$$

$$T_{sp2} = \sum_{n2=1}^{N2} \frac{t_{n2}}{T_s / 2} \tag{3}$$

where

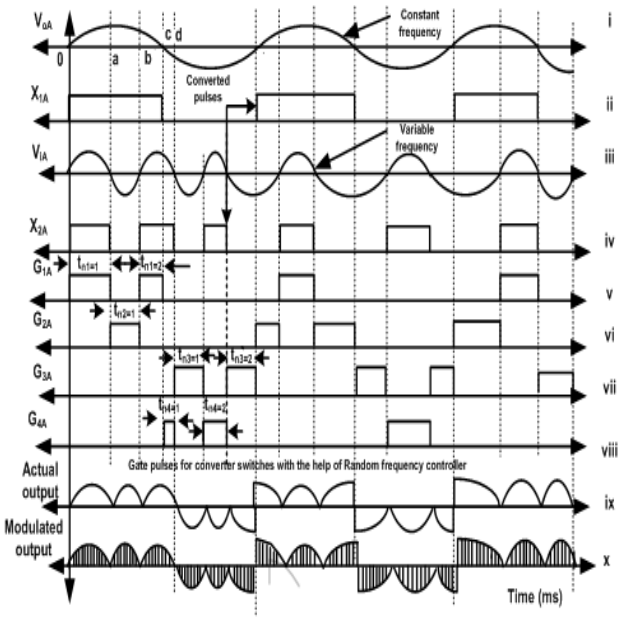

(a)

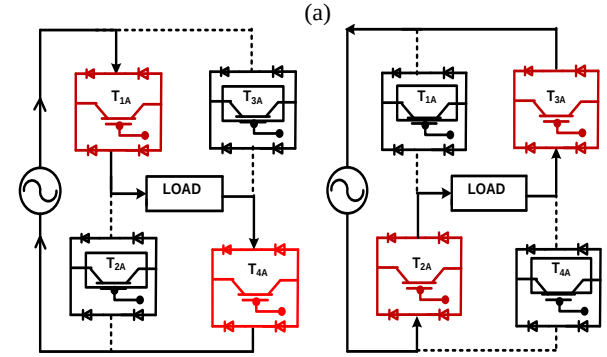

$V_o>0$, $V_i>0$, G_{1A}-(T_{1A}, T_{4A}) $V_o>0$, $V_i<0$, G_{2A}-(T_{2A}, T_{3A})

(b)

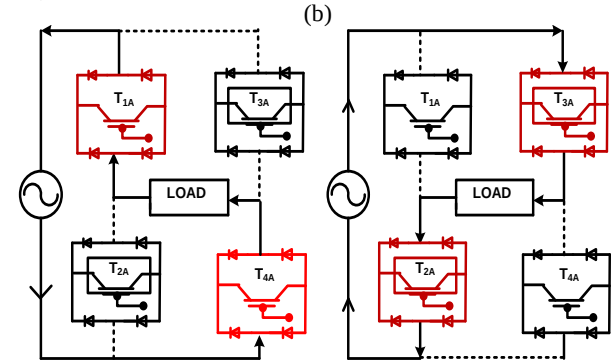

$V_o<0$, $V_i<0$, G_{3A}-(T_{4A}, T_{1A}) $V_o<0$, $V_i>0$, G_{4A}-(T_{3A}, T_{2A})

(c)

Fig. 3. Switching strategy for converter. (a) Gate pulses for variable frequency to constant frequency for AC-AC converter. (b) Converter operation for positive output waveform. (c) Converter operation for negative output waveform.

T_{sp1} and T_{sp2} are the time periods for positive switching period,

N1 and N2 is maximum number of switching pulses obtained for triggering switches T_{1A} & T_{4A} and T_{2A} & T_{3A} in one output half cycle.

T_s is the time period for output waveform, and

t_{n1} and t_{n2} is the duration of the trigger pulses required for triggering switches T_{1A} and T_{4A}, and T_{2A} and T_{3A} in one output half cycle, respectively.

C. Switching Strategy for Negative Output Waveform

The negative half output of the converter is obtained by conducting pair switches (T_{4A} and T_{1A}), and (T_{3A} and T_{2A}), as shown in Fig. 3(c). During time period T_{sn1}, switches T_{3A} and T_{2A} must conduct while the other switches must be turned off; during time period T_{sn2}, T_{4A} and T_{1A} will conduct and the other switches must be turned off. The output voltage for one half negative output cycles is given by Equation (4),

$$V_o = (T_{sn1} - T_{sn2}) \times V_i \tag{4}$$

$$T_{sn1} = \sum_{n3=1}^{N3} \frac{t_{n3}}{T_s / 2} \tag{5}$$

$$T_{sn2} = \sum_{n4=1}^{N4} \frac{t_{n4}}{T_s / 2} \tag{6}$$

where T_{sn1}, and T_{sn2} are the time periods for a negative switching period, and N3 and N4 are the maximum number of switching pulses obtained for triggering the pair switches (T_{3A} and T_{2A}), and (T_{4A} and T_{1A}) in one output half cycle, respectively.

In Fig. 3 (a: ix), the actual output voltage of the converter is distorted and if it is fed to the distributed load system directly, the performance downgrades. To optimize the harmonics in the input and output waveforms, the gate pulses to the different switches are modulated and filtered so that output approaches almost sinusoidal and THD reduces to a minimum value.

The PWM techniques that are used in WECS utilize a carrier wave with a constant switching frequency. If the switching frequency of the carrier frequency is high, the THD and filter size reduce considerably. In this paper, a new approach is adopted where the frequency of the carrier signal is not considered constant but varies according to the wind speed. The intersection of varying frequency carrier waves and reference waves modulate the switching angles of the devices used in the converter to improve the output of the converter is improved and increase the power generated by the turbine. In the next section, a new modified random SPWM approach is discussed in detail.

III. Proposed RSPWM Technique

In the proposed technique, a random sinusoidal reference signal V_{iA} with variable frequency f_i is compared with a high frequency triangular carrier wave of fixed amplitude V_c with variable frequency, as illustrated in Fig. 4. The carrier frequency f_c , of the triangular carrier signal is related with the input supply frequency f_i such that $f_c = f_s \pm k_f$, where, k_f is a frequency multiplier and it takes an integer multiple value of the input frequency. In this application, f_s is the fixed

switching frequency. Thus

$$f_c = f_s \pm k_1 \times f_i \quad (7)$$

The average number of pulses, P, obtained in one cycle by comparing the reference signal and carrier signal is calculated as

$$P = \frac{2\times f_s - k_f}{2\times f_i} \quad (8)$$

Where P is an odd number [23] that meets the following requirements:

1) It is taken in multiples of three to cancel even harmonics.
2) It is normally more than ten.
3) k_1 is always less than 2P.

Thus taking the maximum number of pulses in one cycle, say, equal to 45, the value of k_1 comes out to 30 for a switching frequency of 3 kHz. The pulses of the proposed scheme yield the hybrid characteristics of the random SPWM and random carrier frequency PWM, as shown in Fig. 4(a). This topology is used to reduce the inter-harmonics and sub-harmonics of the converter that are present in the output because of the variation of the input frequency of the turbine-generator system.

The equations for a sinusoidal reference wave with modulation index, M_a and for triangular carrier wave are given by Equations (9) and (10), respectively:

$$V_{iA} = M_a \sin(\omega_r \times t) \quad (9)$$

$$M_p \times \left(t - \frac{\pi\times(i-1)}{2\times M_f} \right) = V_{iA} \quad (10)$$

where,

M_a = modulation index (V_r / V_c),
V_r= magnitude of reference wave,
V_c= magnitude of carrier wave,
M_f = frequency ratio (f_c / f_i),
T=2× π (time period for source),

$M_p = \pm\frac{4\times M_f}{T}$ (slope of triangular wave).

The condition for switching angles is given in Equations (11-12). The equations describing the natural sampled switching instants are transcendental and have the general distinct solutions for odd and even meeting points.

p_i^{th} Intersection (positive slope intersection),

$$t_i + \frac{\pi}{2M_f} M_a \sin(\omega_r \times t_i) - \frac{\pi(i)}{2M_f} = 0 \quad (11)$$

Where, $\frac{4\times(i-1)+1}{4\times M_f}\times T \le t_i \le \frac{4\times(i-1)+3}{4\times M_f}\times T$

p_{i+1}^{th} Intersection (negative slope intersection),

$$t_{i+1} - \frac{\pi}{2M_f} M_a \sin(\omega_r \times t_{i+1}) - \frac{\pi(i+1)}{2M_f} = 0 \quad (12)$$

Where, $\frac{4\times(i-1)-1}{4\times M_f}\times T \le t_{i+1} \le \frac{4\times(i-1)+1}{4\times M_f}\times T$

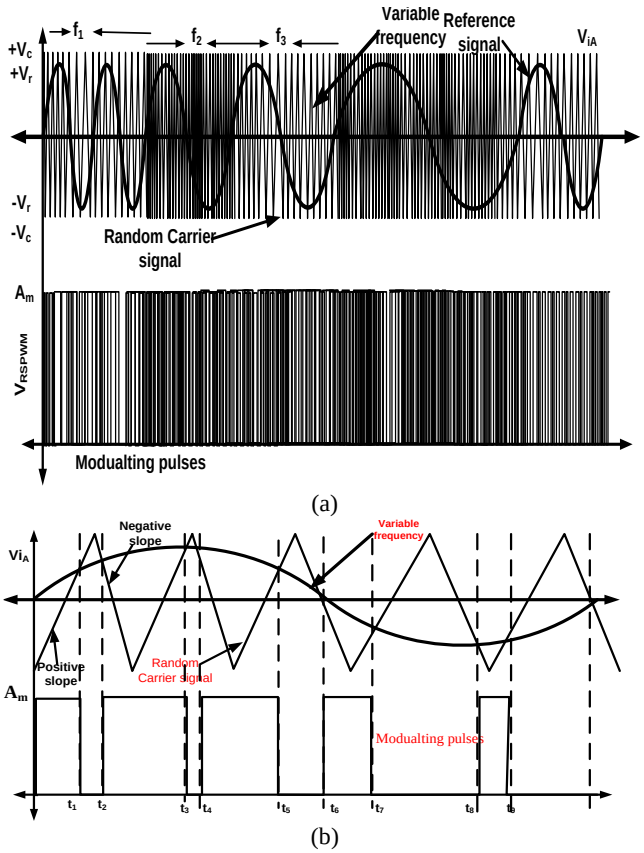

Fig. 4. Switching patterns of RSPWM for phase A. (a) Proposed random sinusoidal PWM technique. (b) Switching state according to random carrier triangular and reference sinusoidal waveform.

The width of the pulse can be obtained by subtracting one odd meeting point from the immediate even successor, as represented by Equation (13). Thus the switching instants and resultant pulse widths for SPWM are analytically represented in Equation (14):

Width of the i^{th} pulse,

$$W_i = t_{i+1} - t_i \quad (13)$$

$$t_n = \left\{ \begin{array}{l} \left(-\frac{\pi}{2M_f} M_a \sin(\omega_r \times t_{i+1}) - \frac{\pi\times(i)}{2M_f} \right) \\ -\left(\frac{\pi}{2M_f} M_a \sin(\omega_r \times t_i) - \frac{\pi\times(i+1)}{2M_f} \right) \end{array} \right\} \quad (14)$$

The switching points may be generalized as (T_{sp1}, T_{sp2}, T_{sn1}, and T_{sn2}) for positive and negative sequences. These modulating points are ANDed with the switching instant in Equation (15),

$$(T_{sp1}, T_{sp2}, T_{sn1}, T_{sn2}) = \left(\left\{ \sum_{n1=1}^{N} \frac{t_{n1}}{T_s/2}, \sum_{n2=1}^{N} \frac{t_{n2}}{T_s/2}, \sum_{n3=1}^{N} \frac{t_{n3}}{T_s/2}, \sum_{n4=1}^{N} \frac{t_{n4}}{T_s/2} \right\} \times \left\{ \sum_{n=1}^{N} \frac{1}{T_s} t_n \right\} \right) \quad (15)$$

Fig. 4(b) shows the switch patterns during the n^{th} time sampling period. The output voltage waveform may follow this path according to operative patterns.

$$V_o = (T_{sp1} - T_{sp2}) \times V_i - (T_{sn1} - T_{sn2}) \times V_i \quad (16)$$

The trigger pulses for the two other converters are generated in a similar manner at a phase difference of 120° and 240^0.

IV. Implementation of Triggering Strategy

The functional diagram for the implementation of the triggering strategy to generate the required constant frequency output with RSPWM is shown in Fig. 5(a). The input signal with variable frequency f_i, is stepped down from a step-down transformer and converted into a square signal using a zero crossing detector (ZCD). The variable frequency signal is generated using Agilent 33220A-20 MHz power supply. The output of ZCD and a reference signal with an output frequency f_o are fed to a de-multiplexer circuit. A zero crossing detector is used to observe the input supply waveform being converted to a digital ON-OFF signal. It consists of a comparator, LM-741, that gives a TTL-compatible output. The de-multiplexer is implemented by a 2×4 decoder. Each channel is dedicated to a particular switch pair. A particular output channel is selected by taking 2 bit word A_1A_0 and decoding it by a 2×4 decoder according to the switching states, as shown in Table I. Depending on the desired output frequency, the multiplexer address is selected. IC 74VHC139 is used as a de-multiplexer that is a high-speed dual 2-to-4 decoder that accepts two binary weighted inputs (A_0–A_1) and provides four mutually exclusive active-LOW outputs (S_1–S_4). Each output of the de-multiplexer has an active-low enable (E). When E is high, all outputs also become high. The enable can be used as the data input for a 4-output de-multiplexer application.

A triangular wave of variable frequency is generated using PLL (LM-566) that is used as a random frequency carrier wave generator. The PLL consists of a phase comparator, amplifier, low pass filter, and Voltage-Controlled Oscillator (VCO), as shown in Fig. 5(b). The phase comparator compares an average control voltage, V_{so}, with the random stepped down sine wave signal V_i. The resulting total control voltage, V_s, is used as the input of the voltage-controlled oscillator to yield a random triangular wave with randomly varied frequencies, as shown in Fig. 4. The voltage-controlled oscillator (VCO) is a circuit that provides a varying output signal whose frequency can be adjusted over a range, controlled by a DC voltage, V_{dc} and set by an external resistor and capacitor to generate a triangular wave. The frequency of carrier wave is given by Equation (17).

$$f_c = \frac{2}{R_1 \times C_1} \times \left(\frac{V_{dc} - V_s}{V_{dc}} \right) \quad (17)$$

The four trigger signals (S_{1A}–S_{4A}) generated at the de-multiplexer's output are ANDed by IC-74HC08 with

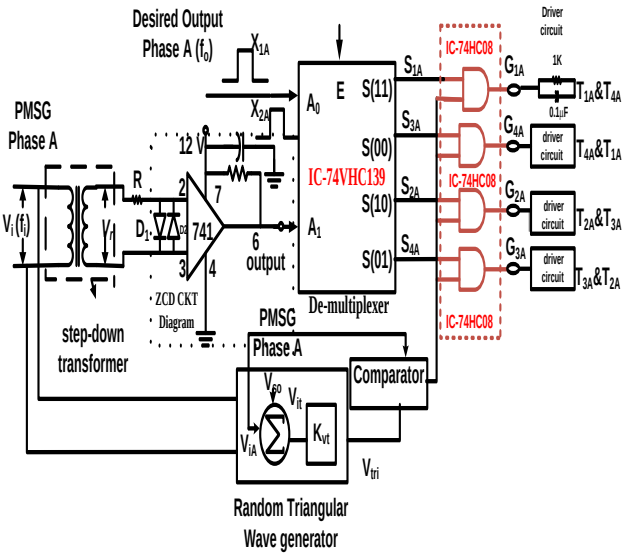

(a)

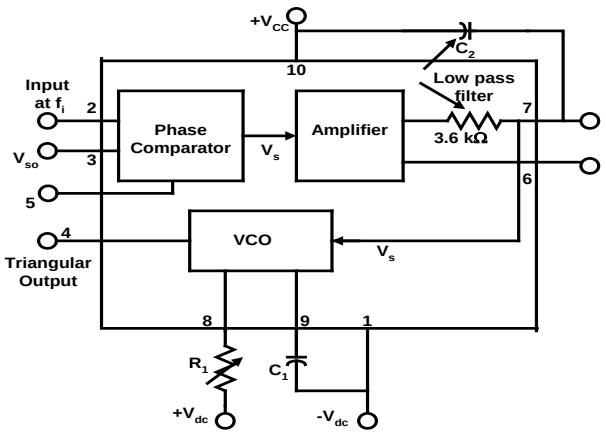

(b)

Fig. 5. Functional diagram for the implementation of a triggering strategy. (a) Proposed frequency controller block diagram for phase A. (b) Detailed circuit diagram of PLL used as a Random Triangular Wave Generator.

modulated output V_{RSPWM} (Fig. 4(a)). The pulses produced at the AND gates are usually at a low power level and boosted to high power level by a driver circuit. A transistor (CL-100) in the driver circuit operates in the active region. The amplified pulses are isolated using opto-coupler 4N35 and fed to the gate of respective IGBTs. The same switching patterns are adapted to operate the converter PB and PC at variable frequency patterns.

V. Simulation Results

The MATLAB/SPS software has been used to simulate the single stage AC–AC converter-based WECS with SPWM and RSPWM. For long durations, the wind behavior may be considered as a combination of ramp, gust, and step and noise behavior. In this manuscript, the wind behavior is listed in Table II.

TABLE II
PARAMETERS FOR THE CONVERTER

Wind speed	5-13 m/s
Output frequency	50 Hz
Input filter inductance & capacitance	5.5 mH, 20 μF
Input damping resistance	40 Ω
Output filter inductance and capacitance	7.95 mH, 20 μF

For short durations, only the step operation is considered. The emphasis is on how the controller works for this condition. However, the controller is also expected to work for other wind patterns. The overall performance of the converter is obtained in both the input supply side and generator side and output load side using the parameters shown in Table II.

A. Input Supply Side Performance

Fig. 6 shows the input voltage and input current as well as the THD performance of the converter for the SPWM technique, where a fixed switching frequency of 3 kHz is used to operate the converter for varying input frequencies of 39–46 Hz. The harmonics in the input currents are lesser when the input frequency f_1 is 46 Hz, whereas when the transition of the input frequency from 46–39 Hz, the harmonics initially increase and subside to an almost negligible value after few seconds. The THD obtained a value of 2.54% and 9.96% for input voltage and input current, respectively, with the SPWM modulation technique along with an input filter, as shown in Figs. 6(a) and 6(b).

When RSPWM technique with an input filter is applied, the harmonics are reduced for both voltage and current. A reduction in THD has been observed at 1.52% and 5.08% for the input voltage and input current, respectively, as shown in Figs. 7(a) and 7(b). Fig. 8 shows the comparative performance of converter for SPWM and RSPWM technique where the switching frequency of 3 kHz is used to operate the converter. Initially, the wind speed is kept at 12 m/s that make the generator/turbine rotate at 200 rpm, as shown in Fig. 8(a). At time t = 0.10 sec, the wind speed decreases to 8 m/s and makes PMSG rotate at 150 rpm. The wind velocity decrement dramatically decreases the input power (Fig. 8(b)) because of the decrease in turbine mechanical power. The active power supplied from the converter reduces from 2.5 pu to 0.8 pu, as shown in Fig. 8(c). The responses of the load active power and the input power are shown for the modified RSPWM technique, as seen in Figs. 8(b)-(c), respectively. The output power increased compared with the conventional SPWM technique. In the RSPWM, the average output power increased to approximately 5% to 10 % compared with the SPWM technique.

Further reduction in the THD for input current and input voltage can be obtained by increasing the frequency of the carrier wave, as shown in Table III that illustrates the impact of switching frequency on the THD of system. For a fixed

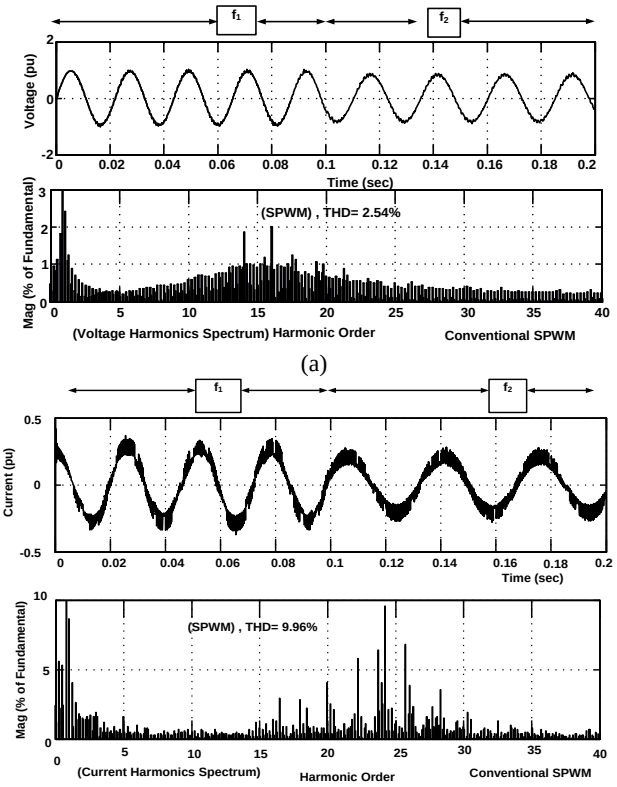

Fig. 6. Input performances of converter with SPWM. (a) Input Voltage waveform and harmonic spectrum. (b) Input current waveform and harmonic spectrum.

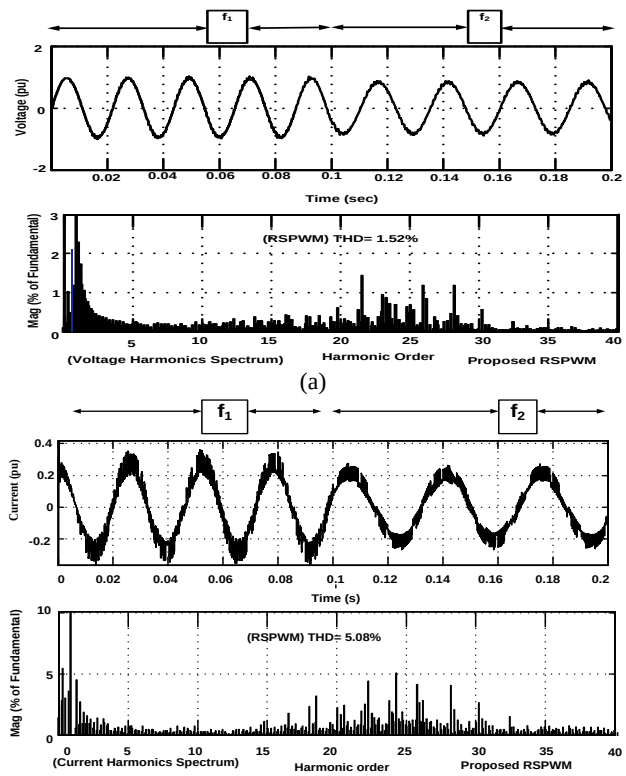

Fig. 7. Input Performances of converter with RSPWM. (a) Input voltage waveform and harmonic spectrum. (b) Input current waveform and harmonic spectrum.

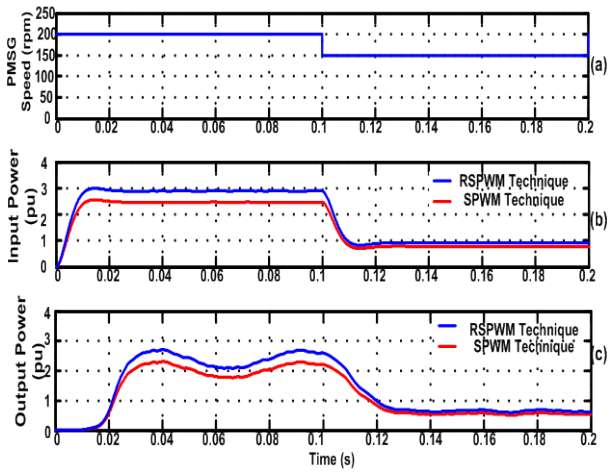

Fig. 8. Performance of AC-AC converter.

TABLE III
IMPACT OF SWITCHING FREQUENCIES ON THE THD OF THE SYSYEM

S.N	Filter size		Switching frequency (kHz)	Input side: THD of system	
	Inductor L (µH)	Capacitor C (µF)		Voltage (%)	Current (%)
1	2000	20	4	7.64	4.68
2			6	6.32	3.48
3			8	6.01	2.76

input filter size, the THD of the current and voltage reduces when the switching frequency is increased.

B. Load Side Performance

The presence of the harmonic components in the voltage and current affect the power quality and efficiency of the converter because of the nonlinearity of the power switches (IGBTs). The output voltage of the converter can be improved further by the addition of an LC filter at a cutoff frequency equal to 850 Hz that is greater than 10 to 20 times the fundamental frequency and lower than 10 to 15 times the switching frequency [23]. A 20 µF capacitor and 7.95 mH inductor are used to mitigate the higher order harmonics of the system. Fig. 9(a) shows the output performance of the converter with SPWM without using any filter. Fig. 9(b) illustrates the converter performance with a filter and the SPWM technique. The modulation technique reduces the lower order harmonic magnitude; whereas the higher order harmonics are compensated with the help of LC filter. Without using any filter, the output of THD is very high with a value of approximately 70.4% and is reduced to 18.4% after inserting an LC filter in the output power circuit.

Fig. 9(c) depicts that the output current of the converter tends to be sinusoidal. The output performance of the converter with RSPWM is illustrated in Fig. 10. Without using any filter, the THD is 54.4%, and is less than the value obtained with the SPWM. With a filter, the THD is reduced by approximately 50%, as shown in Figs. 10(b) and 10(c).

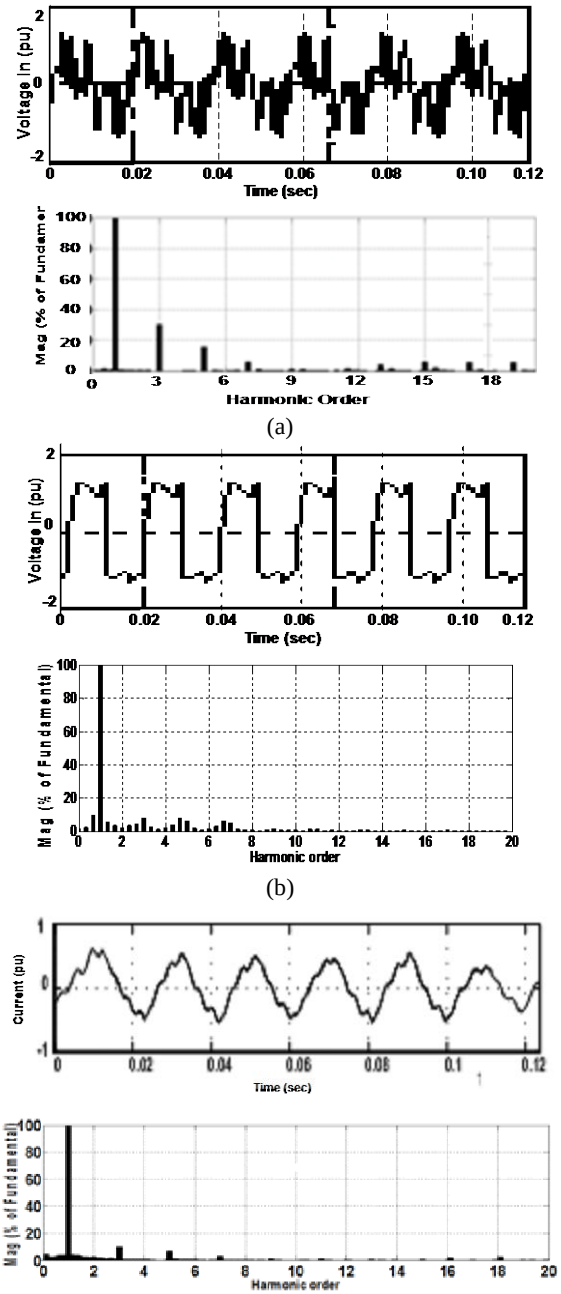

Fig. 9. Output performance of the converter with the SPWM. (a) Output voltage and harmonic spectrum with SPWM. (b) Output voltage and harmonic spectrum with SPWM and L-C filter. (c) Output current waveform and harmonic spectrum with SPWM and L-C filter.

A prototype of the proposed AC-AC converter is developed in the lab to verify the results. Fig. 11 shows the photo of the experimental set-up that includes an input interfacing circuit consisting of step-down transformer and zero crossing detector (ZCD), trigger circuit, driver circuit, isolation circuit, and power circuit made up of IGBTs (BUP 314D) with an ultra-fast soft recovery diode. The 220 V rms variable frequency supply is used with a low pass LC filter, 5.5 mH inductor, and 20 µF capacitor. The input transformer

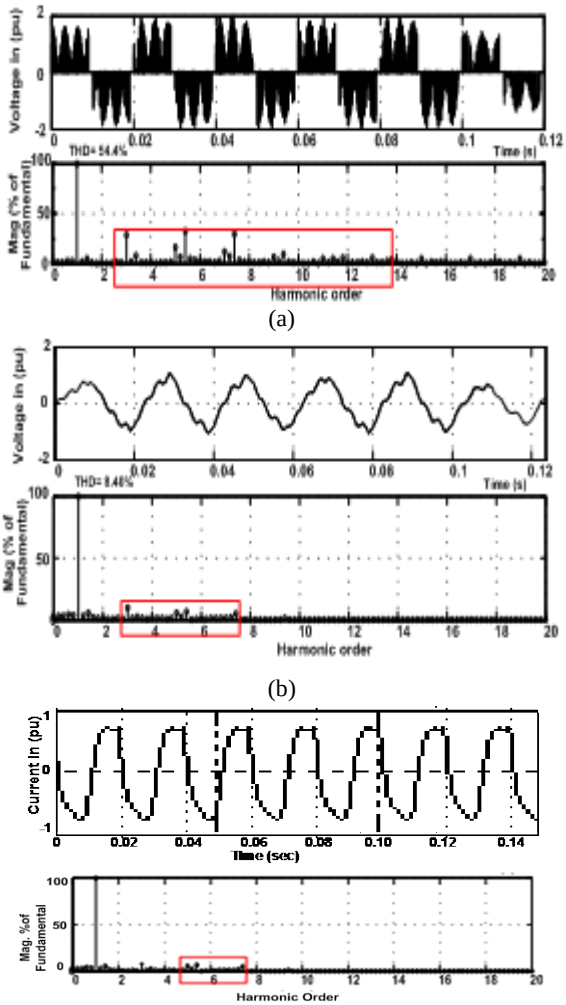

Fig. 10. Output Performance of Converter with RSPWM. (a) Output voltage waveform and harmonic spectrum with RSPWM. (b) Output voltage waveform and harmonic spectrum with RSPWM and L-C filter. (c) Output current waveform and harmonic spectrum with RSPWM and L-C filter.

rating is given by $V_{rms} \times I$, where V_{rms} and I are the rated voltage and current of the transformer that are 220 V and 5A, respectively. The input transformer rating is equal to 1100 VA. If the power factor is assumed to be 0.9, the output power of transformer P_i is equal to $1100 \times 0.9 = 990$ W. Thus the maximum power of 990 W may be transferred to grid in the experiment.

VI. Experimental Results

The basic trigger signal for IGBTs ($T_{1A,}$ T_{4A}), and ($T_{2A,}$ T_{3A}) are generated at the de-multiplexer's output as shown in Fig. 12(a).

Fig. 12(b) exhibits the random carrier signal and random reference pulse. These two signals are compared in a comparator to obtain the required time resolution pulses as shown in Fig. 12(c). The basic signals are ANDed with

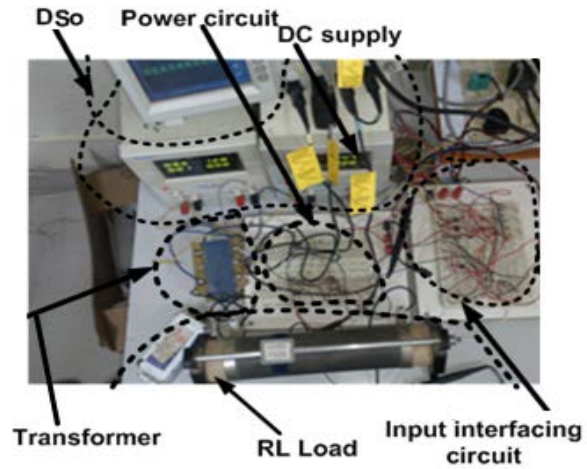

Fig. 11. Experimental Set-up.

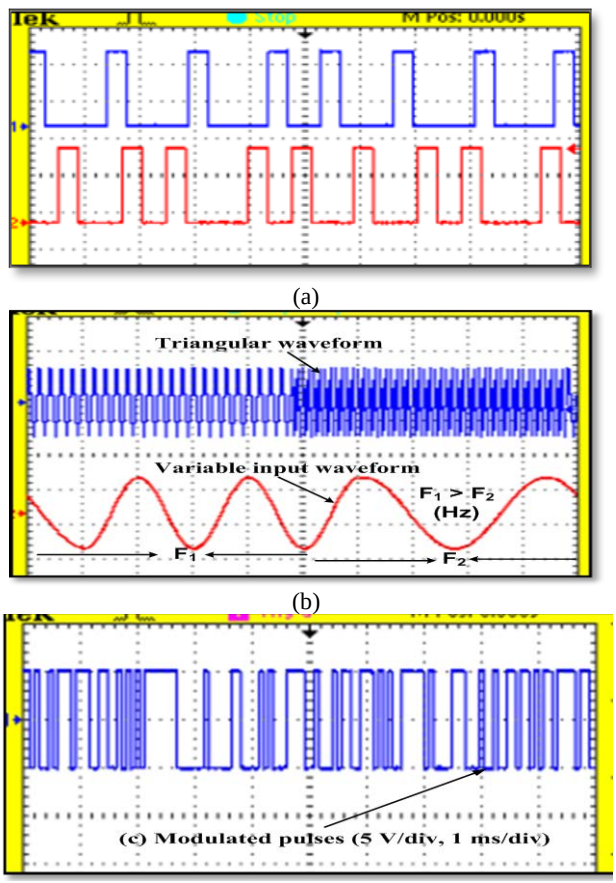

Fig. 12. Pulse generation for AC-AC converter. (a) Pulses for T_{1A}-T_{4A} (upper trace) and T_{2A}-T_{3A} (lower trace) (5V/div, 5 ms/div). (b) Triangular waveform (upper trace: 5 V/div, 12 ms/div) and input waveform (lower trace: 5 V/div, 12 ms/div). (c) Modulated pulses for (lower trace: 5 V/div, 1 ms/div)

modulated output and fed to the gate of respective IGBTs through driver circuits. The combined trace of input and output voltage waveforms of the module is shown in Fig. 13. The highly distorted, un-modulated output of the converter is depicted in Fig. 13(a). Fig. 13(b) exhibits the output with the

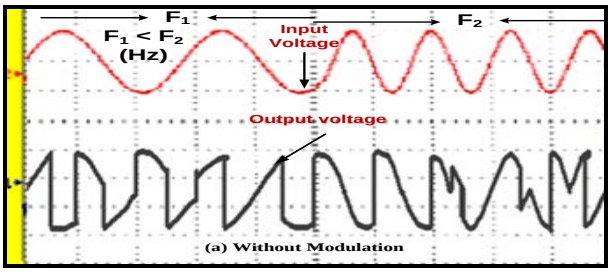

(a)

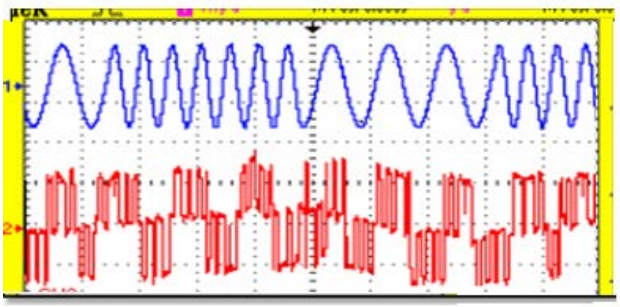

(b)

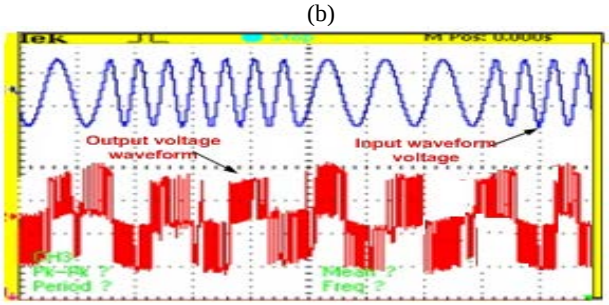

(c)

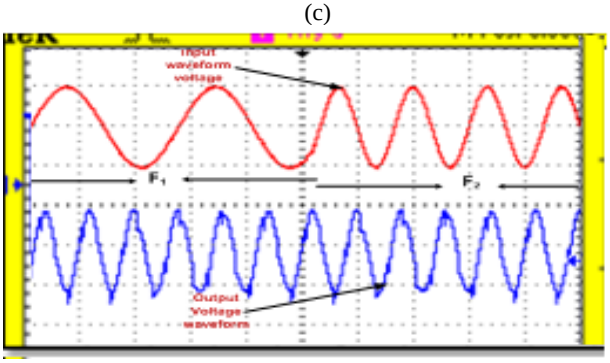

(d)

Fig. 13. Input Voltage of Varying frequency and output voltage for constant frequency of 50 Hz. (a) Input Voltage (upper trace: 100V/div, 20 ms/div) & output voltage (lower trace: 50V/div, 20 ms/div) without modulation. (b) Input voltage V_i (upper trace: 100V/div, 10 ms/div) & output voltage V_o (lower trace: 50V/div, 10 ms/div) with SPWM. (c) Input voltage (upper trace: 100V/div, 10 ms/div) & output voltage (lower trace: 50V/div, 10 ms/div) with RSPWM. (d) Input voltage (upper trace: 100V/div, 20 ms/div) & output voltage (lower trace: 50V/div, 10 ms/div) with LC filter.

conventional SPWM, whereas Fig. 13(c) shows the converter output with RSPWM. Frequent turning ON and OFF of the IGBTs is needed because the number of pulses per half cycle is larger in Fig. 13(c) than in Fig. 13(b). The output with the RSPWM and LC filter is depicted in Fig. 13(d). A constant

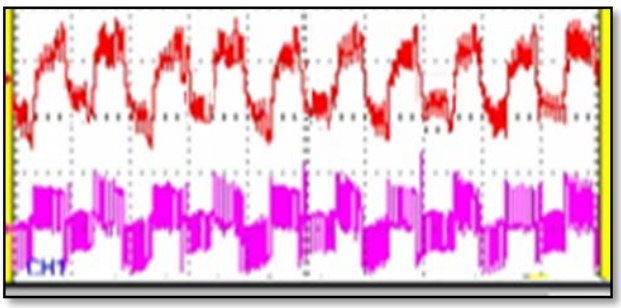

(a)

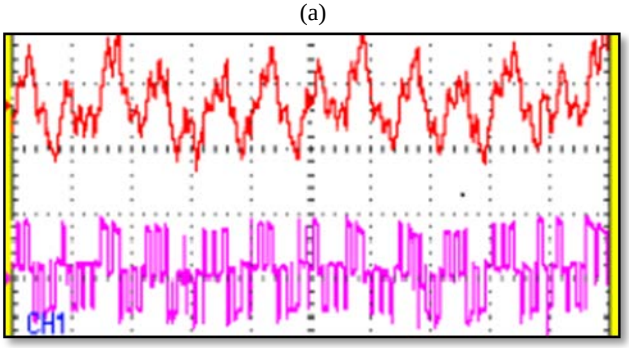

(b)

Fig. 14. Output Voltage and Grid Current. (a) Output Current I_o (upper trace: 1 A/div, 20ms/div) & Output voltage V_o (lower trace: 50V/div, 20 ms/div) with RSPWM. (b) Output Current I_o (upper trace: 1 A/div, 20ms/div) & Output voltage V_o (lower trace: 50V/div, 20 ms/div) with SPWM.

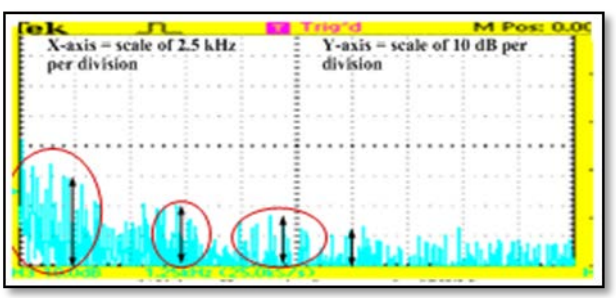

(a)

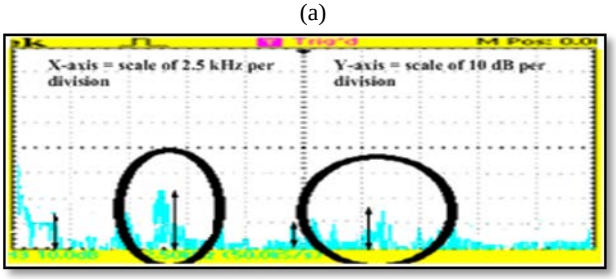

(b)

Fig. 15. FFT of input voltage. (a) Voltage harmonics spectrum for SPWM. (b) Voltage harmonics spectrum for RSPWM.

output frequency of 50 Hz is achieved in almost all cases. Fig. 14 shows the output voltage and grid current for SPWM and RSPWM. The current waveform tends to be more sinusoidal in Fig. 14(a) with RSPWM as compared to Fig. 14(b) with SPWM.

The harmonic spectrum of the input voltage for SPWM at

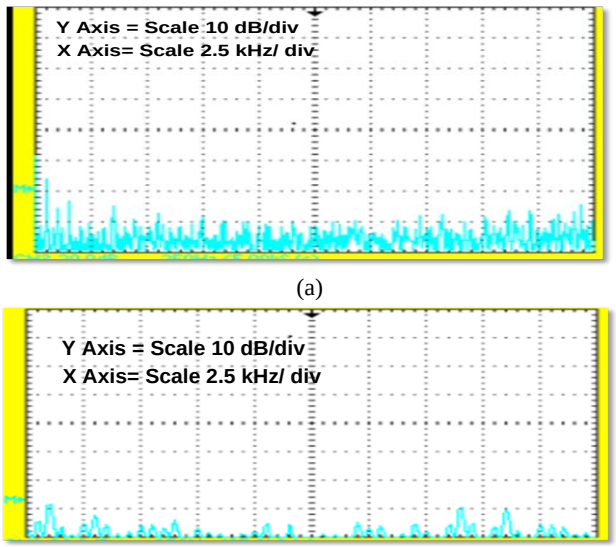

Fig. 16. FFT of output voltage of converter. (a) Voltage harmonics spectrum for SPWM. (b) Voltage harmonics spectrum for RSPWM.

a 3-kHz fixed frequency is shown in Fig. 15(a). The most dominant harmonics of voltage is placed around the switching frequency (3 kHz), whereas the residuary harmonics are spread around the switching frequency. In RSPWM, the most dominant harmonics of voltage is placed around the switching frequency; the residuary harmonics are minimized as shown in Fig. 15(b). The harmonic spectrum of the output voltage for SPWM and RSPWM is shown in Fig. 16. Comparisons for Fig. 6 and Fig. 7 with Fig. 15 and Fig. 9, and Fig. 10 with Fig. 16, the harmonic spectrum has been found to be much better in the RSPWM compared with the SPWM. Simulation and experimental results verify these findings.

VII. Conclusions

A single stage AC-AC converter has been designed for WECS that changes the variable input frequency of PMSG to a constant output frequency fed to the grid/load. A new modulation technique, RSPWM, has been developed where the frequency of the carrier wave is not considered constant but varies randomly in proportion to the wind speed. The frequency of the reference wave also varies. The intersection of the reference waveform and carrier waveform modulates the firing angles of the switches to increase the output power generated by the turbine by approximately 5%–10% compared with the conventional SPWM technique. The THD of both input current and input voltage of converter is also reduced by 40% compared with the conventional SPWM technique. Load voltage improves when this technique is applied with a constant LC filter. The simulated results are verified by experimental results, and are consistent with each other.

References

[1] N. Singh and V. Agarwal, “A review on power quality enhanced converter of permanent magnet synchronous wind generator,” *International Review of Electrical Engineering (IREE)*, Vol. 8, No. 6, pp. 1681-1693, Nov. 2013.

[2] R. Melicio, V. M. F. Mendes, and J. P. S. Catalao, “Power converter topologies for wind energy conversion systems: Integrated modelling, control strategy and performance simulation,” *Renewable Energy*, Vol. 35, No. 10, pp. 2165-2174, Oct. 2010.

[3] A. V. Santiago and I. V. Maria, “Direct connection of WECS system to the MV grid with multilevel converters,” *Renewable Energy*, Vol. 41, pp. 336-344, May 2012.

[4] N. A. Orlando, M. Liserre, V. G. Monopoli, R. A. Mastromauro, and A., DellAquila, “Comparison of power converter topologies for permanent magnet small wind turbine system,” *Industrial Electronics, 2008. ISIE 2008. IEEE International Symposium on*, pp.2359-2364, 2008.

[5] T. Ahmedy, K. Nishida, and M. Nakaoka, “Wind power grid integration of an IPMSG using a diode rectifier and a simple MPPT control for grid-side inverters,” *Journal of Power Electronics*, Vol. 10, No. 5 , pp. 548-554, Sep. 2010.

[6] T. Friedli, J. W. Kolar, J. Rodriguez, and P. W. Wheeler, “Comparative evaluation of three-phase AC–AC Matrix converter and voltage DC-link back-to-back converter systems,” *IEEE Trans. Ind. Electron*., Vol. 59, No. 12, pp. 4487-4510, Dec. 2012.

[7] H. J. Cha and P. N. Enjeti, “A three-phase AC/AC high-frequency link matrix converter for VSCF applications,” *Power Electronics Specialist Conference*, Vol. 4, pp. 1971-1976, 2003.

[8] M. N. Marwali, D. Min, and A. Keyhani, “Robust stability analysis of voltage and current control for distributed generation systems,” *IEEE Trans. Energy Convers*., Vol. 21, No. 2, pp.516-526, Jun. 2006.

[9] I. Vechiu, O. Curea, and H. Camblong, “Transient operation of a four-leg inverter for autonomous applications with unbalanced Load,” *IEEE Trans. Power Electron.*, Vol. 25, No. 2, pp. 399-407, Feb. 2010.

[10] M. Singh, V. Khadkikar, A. Chandra, and R. K. Varma, “Grid interconnection of renewable energy sources at the distribution level with power-quality improvement features,” *IEEE Trans. Power Del*., Vol. 26, No. 1, pp. 307-315, Jan. 2011.

[11] R. Cardenas, R. Pena, P. Wheeler, J. Clare, and C. Juri, “Control of a matrix converter for the operation of autonomous systems,” *Renewable Energy*, Vol. 43, pp. 343-353, Jul. 2012.

[12] J. Rodriguez, M. Rivera, J. W. Kolar, and P. W. Wheeler, “A review of control and modulation methods for matrix converters,” *IEEE Trans. Ind. Electron*., Vol. 59, No 1, pp. 58-70, Jan. 2012.

[13] S. Gupta and V. Agarwal, “An efficient algorithm for single phase converter,” *IET Power Electron.*, Vol. 3, No. 1, pp. 138-145, Jan. 2010.

[14] T. Senjyu, S. Tamaki, E. Muhando, N. Urasaki, H. Kinjo, and T. Funabashi, “Wind velocity and rotor position sensor less maximum power point tracking control for wind generation system,” *Renewable Energy*, Vol. 31, No. 11, pp. 1764-75, Sep. 2006.

[15] C. Xia, J. Zhao, Y. Yan, and T. Shi, “A novel direct torque control of matrix converter-fed PMSM drives using duty cycle control for torque ripple reduction,” *IEEE Trans. Ind. Electron*., Vol. 61, No. 6, pp. 2700-2713, Jun. 2014.

[16] R. B. Kumar and A. N. Kumar, "Performance analysis of wind turbine-driven permanent magnet generator with matrix converter," *Turkish Journal Electrical Engineering & Computer Science*, Vol. 20, No. 3, pp. 299-317, May 2012.
[17] C. Ponmani and M. Rajaram, "Compensation strategy of matrix converter fed induction motor drive under input voltage and load disturbances using internal model control," *International Journal of Electrical Power & Energy Systems*, Vol. 44, No. 1, pp. 43-51, Jan. 2013.
[18] K. Yang, M. H. J. Bollen, E. O. A. Larsson, and M. Wahlberg, "Measurement of harmonic emission versus active power from wind turbines," *Electric Power Systems Research*, Vol. 108, pp. 304-314, Mar. 2014.
[19] S. T. Tentzerakis and S. A. Papathanassiou, "An investigation of the harmonic emissions of wind turbines," *IEEE Trans. Energy Convers.*, Vol. 22, No. 1, pp. 150-158, Mar. 2007.
[20] B. Wang and E. Sherif, "Spectral analysis of matrix converters based on 3-D fourier integral," *IEEE Trans. Power Electron*., Vol. 28, No. 1, pp. 19-25, Jan. 2013.
[21] M. E. Haque, M. Negnevitsky, and K. M. Muttaqi, "Novel control strategy for a variable-speed wind turbine with a permanent-magnet synchronous generator," *IEEE Trans. Ind. Appl*., Vol. 46, No 1, pp. 331-339, Jan./Feb. 2010.
[22] A. Agarwal and V. Agarwal, "FPGA based variable frequency AC to AC power conversion," *Electric Power Systems Research*, Vol. 90, pp. 67-78, Sep. 2012.
[23] H. Cha and T.-K. Vu, "Comparative analysis of low-pass output filter for single-phase grid-connected Photovoltaic inverter," in *Proc. Applied Power Electronics Conference and Exposition (APEC)*, pp. 1659-1665, 2010.

Navdeep Singh was born in Pratapgarh, India on March 22, 1987. He graduated from the Uttar Pradesh Technical University, Lucknow, India with B.Tech degree in Electrical Engineering in 2009 and completed his M.Tech in Power Electronics and ASIC Design at MNNIT, Allahabad in July 2011. He is working as Research Scholar in Electrical Engineering Department, NIT Allahabad, and Uttar Pradesh, India. His research interests include wind energy, power electronic devices, converters, and AC to AC converter.

Vineeta Agarwal graduated from Allahabad University, Allahabad, India, in 1980, and received her Master's degree in 1984, from the same university. She joined the Electrical Engineering Department at the MOTILAL Nehru Regional Engineering College, Allahabad, India as lecturer in 1982. While teaching there, she obtained her Ph.D. in Power Electronics. At present she is a Professor in the Department of Electrical Engineering at the MOTILAL Nehru National Institute of Technology, Allahabad, India. She has taught numerous courses in Electrical Engineering and Electronics. Her research interests are in single phase to three-phase conversion and AC drives. She has a number of publications in journals and conferences in her field. She has attended and presented papers at both national and international conferences.